Association between a Failed Prominence Eruption and the Drainage of Mass from Another Prominence*

Jian-chao Xue**, Li Feng, Ping Zhang, ASO-S/LST team @ PMO, CAS, China

Abstract. We present a failed prominence eruption and subsequent mass drainage from a distinct prominence and explore their causal links. Using stereoscopic observations including *ASO-S/LST*, *CHASE*, and *Solo/EUI*, we observe the north prominence (PRO-N) rising up following the south prominence (PRO-S), and its upper part vanishes due to catastrophic mass draining along an elongated structure. Observations suggest that the elongated structure connecting PRO-N overlies PRO-S, which causes the rising up of PRO-N along with PRO-S and mass drainage after PRO-S eruption. We propose that a prominence may end its life through catastrophic mass drainage, where rising and mass drainage strengthen each other, and mass drainage can be initiated by an eruption underneath.
In addition, we derived physical quantities of PRO-S with Lyα and Hα intensities and Hα FWHM using 1D NLTE modeling. With the PRODOP code available at MEDOC (IAS), we firstly studied the effects of prominence temperature, pressure, thickness, microturbulence velocity, height, and bulk velocity on emergent spectra. Then relationships between radiative and prominence quantities were built through more than 500 000 isothermal and isobaric models, through which we could derive PRO-S temperature and densities.

Eruption Overview

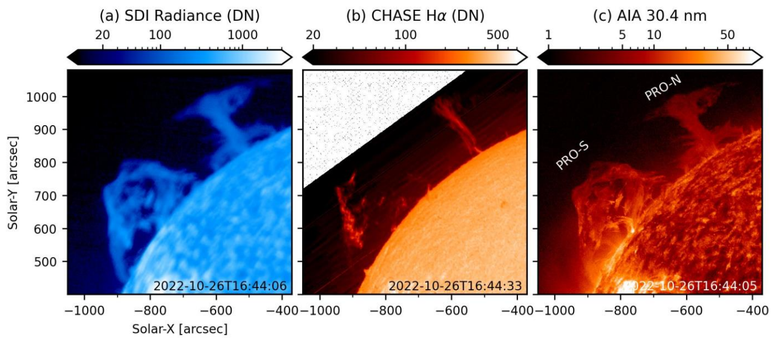

Fig. 1 Prominence images of SDI Lyα, CHASE Hα, and AIA 30.4 nm. There are two prominences named as PRO-S and PRO-N.

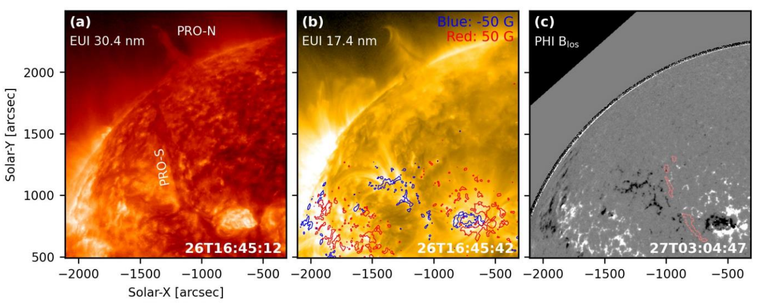

Fig. 2 Prominence images in Solo view by EUI and PHI. Contours in (b) represent B_{los} of 50 G. In (b), there is a horn-like structure at top of PRO-N.

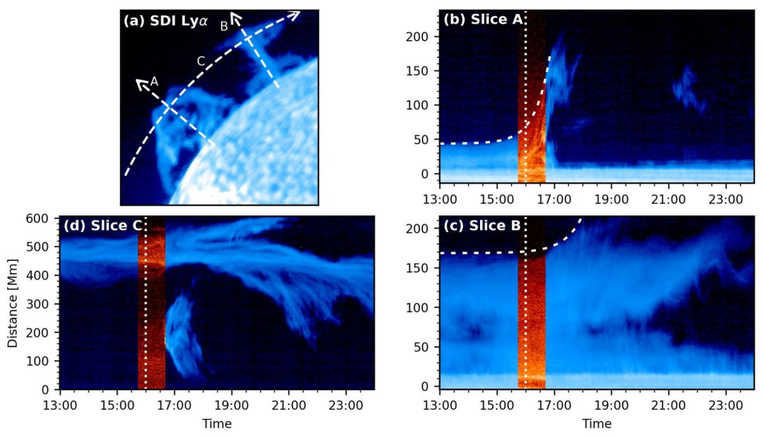

Fig. 3 Time–distance diagrams of prominence eruptions in Lyα (blue) and 30.4 nm (red). We can see (1) PRO-S rises up preceding PRO-N, (2) PRO-N is pushed away during PRO-S rising.

PRO-S Failed Eruption

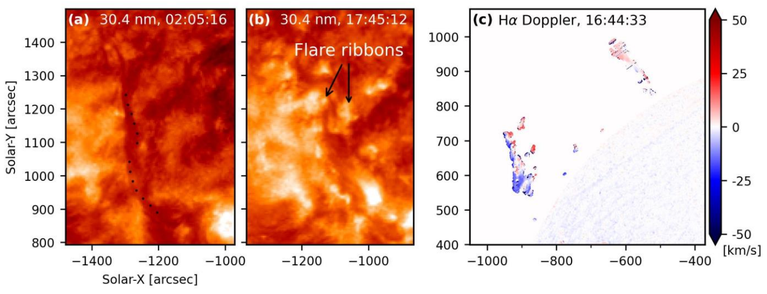

Fig. 4 Cause of PRO-S eruption initiation. (a) PRO-S is a winding structure. (b) Flare ribbons occur following PRO-S eruption. (c) Untwisting motion is indicated from Hα Doppler image.

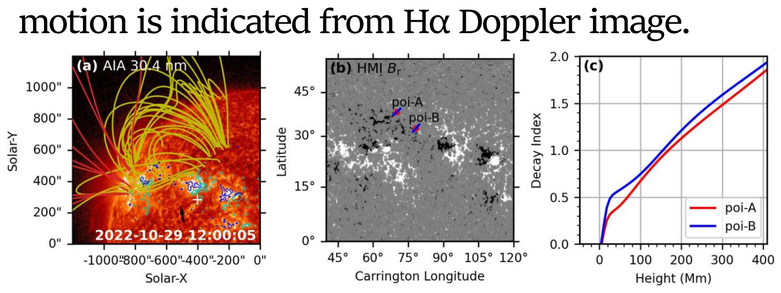

Fig. 5 Potential-field configuration and decay index. At the height of PRO-S disappearance, the decay index is around 1.1, suggesting background field does not provide a strong upward force.

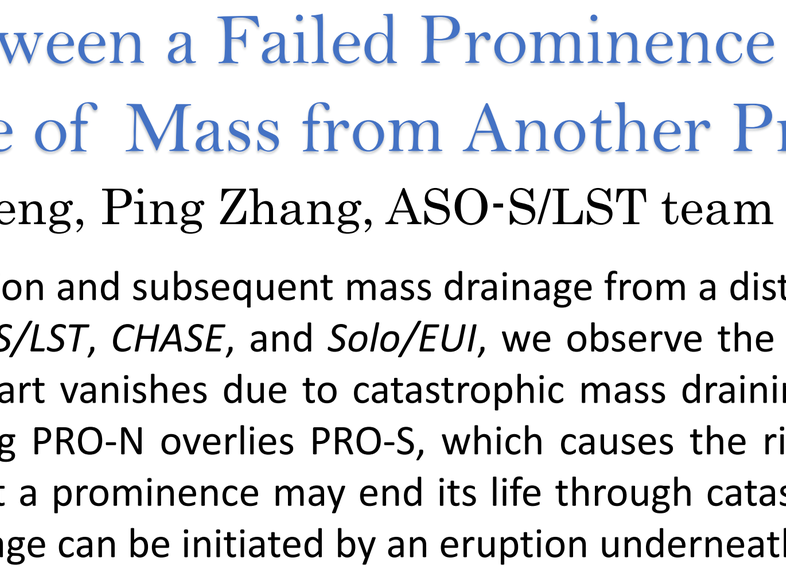

Fig. 6 Process of the PRO-S failed eruption. New connections are found (marked by pink arrows), which suggests that external reconnection occurs and contributes to the failed eruption.

PRO-N Mass draining

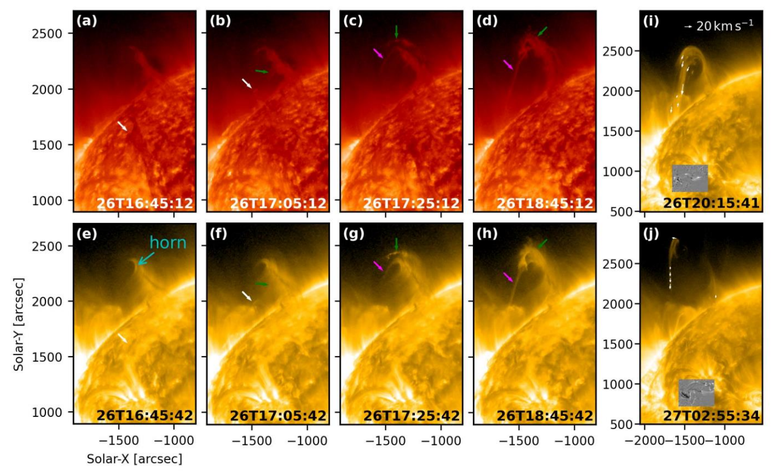

Fig. 7 PRO-N mass draining in EUI view. After PRO-S failed eruption, mass drainage from PRO-N starts along the horn structure (d&h). At the same time, brightening is found at a region on the disk (i-j). It suggests that the horn structure may connect with this region, and is over PRO-S.

Catastrophic mass drainage: rising and mass drainage strengthen each other, until the prominence disappears.

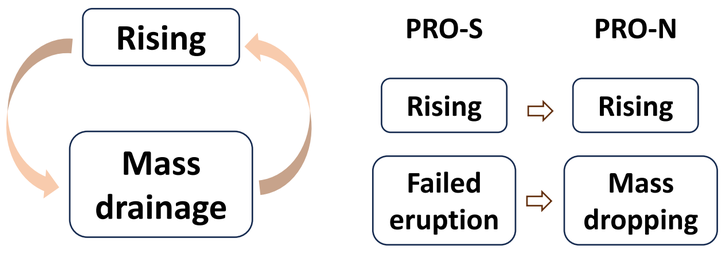

Conclusion

- PRO-S rises under kink instability and flare reconnection, followed by PRO-N rising;
- PRO-S failed due to external reconnection;
- PRO-N catastrophic mass drainage is triggered due to PRO-S failed eruption.

What's New:

- Catastrophic mass drainage;
- Large-scale connection of the prominence horn;
- A failed eruption triggers mass drainage of another prominence.

Spectral inversions

With imaging observations of SDI Lyα and spectral and imaging observations of CHASE Hα, we could derive physical quantities of PRO-S using Lyα and Hα intensities, Hα FWHM, altitude, and bulk velocity in Sun-radial direction. The bulk velocity was calculated using an optical-flow method.

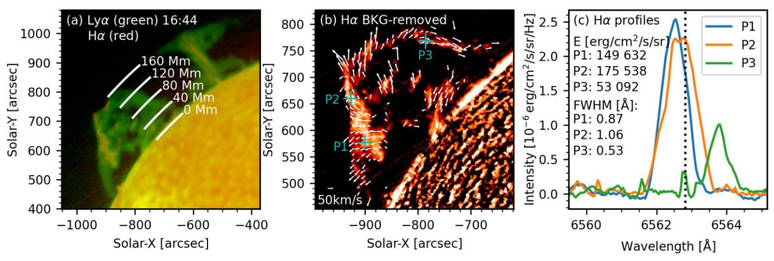

Fig. 8 Observation parameters. (a) Composite image of Lyα (green) and Hα center (red). (b) Image of Hα integral intensity with background (an image after the eruption) removed. (c) Hα profiles at points marked in (b).

The 1D NLTE code PRODOP was used to derive the relationships between radiative and atmospheric quantities. Before that, effects of input parameters of isothermal and isobaric prominence models on emergent spectra were checked.

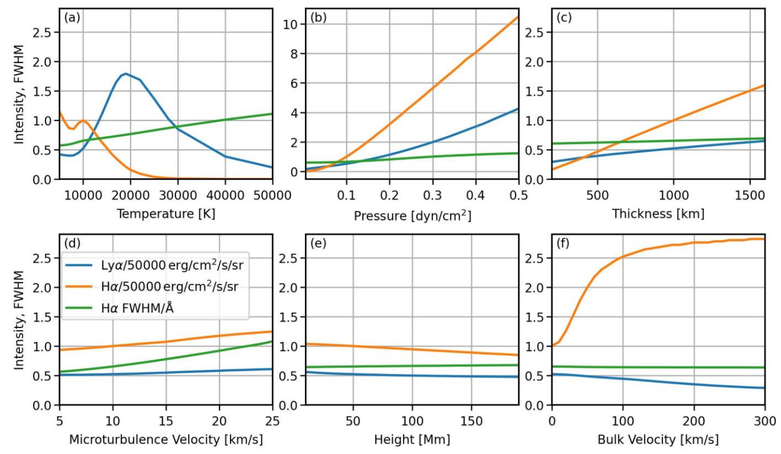

Fig. 9 Basic input parameters are temperature 10 000 K, pressure 0.1 dyne/cm², thickness 1000 km, microturbulence velocity (v_{tur}) 10 km/s, height 50 Mm, bulk velocity 0 km/s. The results suggest that temperature larger than 25 000 K is not necessary, pressure has significant effects, thickness affects Hα intensity obviously, v_{tur} mainly affects Hα width, height has a weaker effect, and bulk velocity affects Hα intensity significantly.

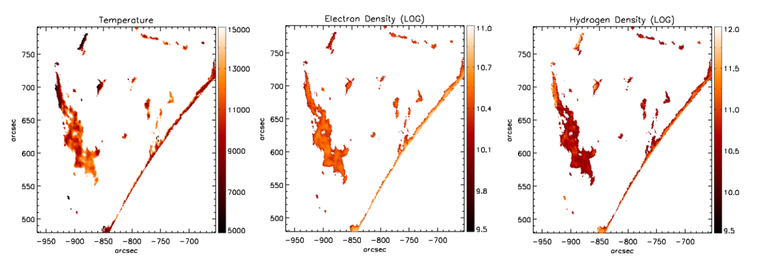

Fig. 9 Preliminary results derived with varying temperature, pressure, and altitude. With more parameters considered, better spectral-inversion results are expected.

*Solar Physics, 2024, 299, 89
**xuejc@pmo.ac.cn